IEEE Access
Multidisciplinary | Rapid Review | Open Access Journal

Received September 3, 2019, accepted October 8, 2019, date of publication October 18, 2019, date of current version October 30, 2019.

Digital Object Identifier 10.1109/ACCESS.2019.2948378

Research on a New-Style Under-Actuated Omnidirectional Mobile Robot Based on Special Coupling Drive System

ZHIGUO LU[1], MENGLEI LIN[1], SHIXIONG WANG[1], YICHEN ZHANG[1], AND YONGJI YU[1,2]
[1]School of Mechanical Engineering and Automation, Northeastern University, Shenyang 110819, China
[2]Huawei Technologies Company Ltd., Shenzhen 518129, China

Corresponding author: Menglei Lin (1778645865@qq.com)

This work was supported by the National Key R&D Program of China (2018YFB1304504), National Natural Science Foundation of China (51505069), together with Fundamental Research Funds for the Central Universities (N150308001).

ABSTRACT In some existing omnidirectional mobile robots, the movement of each wheel is generally controlled by one driven motor cooperates with one steering motor, such design will increase the energy consumption. This paper investigates an omnidirectional mobile robot based on a special coupling system, so as to solve the above problem. We propose a unique robot's steering method by designing the parallelogram connecting rod as the coupling system, which makes each wheel only need to be equipped with one motor to complete omnidirectional motion and always keep unchanged robot's attitude. In theory, we conduct the structural analysis, dynamic analysis and kinematic analysis of the mobile robot and explain why our system is under-actuated. In experiments, the square trajectory and the serpentine trajectory are exploited to verify the rationality of design and theoretical derivation by comparing the simulation results with the experimental results. By performing mobile robot walking experiments under different ground condition respectively, the stability and adaption of the under-actuated omnidirectional mobile robot is also favourably confirmed. After detailed theoretical analysis and the support of experiments, it is carried out that the under-actuated mechanism proposed in this paper can indeed realize the movement of the robot in all directions. As well as the attitude of the robot always keeps constant, as we expected, enables to realize the steering of robot flexibly even in a narrow space.

INDEX TERMS Constant attitude, mobile robot, omnidirectional, under-actuated.

I. INTRODUCTION

In recent years, with the rise of artificial intelligence technology, the robots have been applied to several fields. Such as the climbing robots for detecting tasks [1], [2], mobile robots that can be used in home and industrial environments [3]. Particularly, mobile robot as an important branch of robotics has received a great attention by most countries [4]. The earliest appeared is the wheeled robot developed by Stanford, which is primarily capable of self-service reasoning, planning and control in complex environments [5]. As time goes by, the relevant researches on mobile robots are also deepening with the assistance of advanced technology. A mass of omnidirectional mobile robots have been applied widely due to the emergence of omnidirectional wheel technology. In order to meet the use of mobile robots in different scenarios, the choice of wheel mechanism is particularly important [3]. Among them, the design scheme of Mecanum wheel is proposed in 1973 and is subsequently exploited [6], [7]. In [8], presents an omni-directional mobile robot using four custom-made mecanum wheels, each wheel is independently powered using a precisian gear DC motors. The KUKA company in Germany takes full advantage of its own robot development and launches the YouBot robot into people's view [9], [10]. Subsequently, KUKA introduces the omniMove large mobile robot platform, which has flexible mobility and powerful load capacity despite its bulk [11]. Because of the structural characteristics of the Mecanum wheel, the diameter and width are limited [12] and the discontinuity of contact points results the introduction of vibrations into the base [13]. On this account, it cannot tolerate too large loads and has erratic motion on the uneven ground.

The associate editor coordinating the review of this manuscript and approving it for publication was Min Wang.

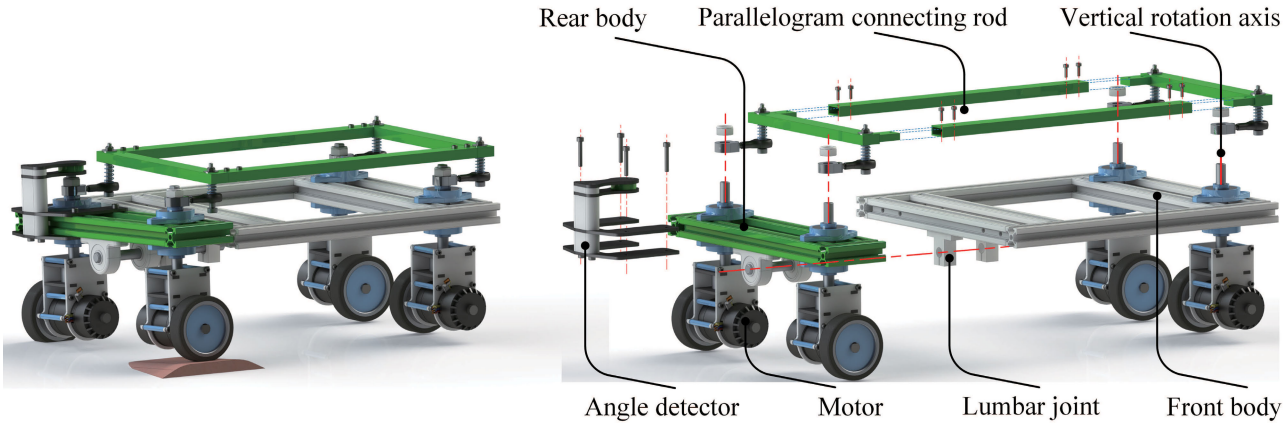

FIGURE 1. The integral model diagram (left) and the splitting diagram (right) of the under-actuated omnidirectional mobile robot.

In addition, the ordinary wheel of most structures is equipped with at least double motors and one motor drives the roller to roll, the other motor drives the roller to steer [14], [15], which realizes the omnidirectional movement of the robot [16]. Such as, MIT has designed a ordinary wheeled omnidirectional mobile robot, whose travel mechanism consists of two wheels that are symmetrically mounted on either side of the vertical rotation axis. A single set of travel mechanism uses two motors to control walking and steering separately, enabling the robot to achieve omnidirectional movement on the ground [17]. Following, the company of MobileRobots has also developed a mobile sweeping robot by Dumitrascu *et al.* [18], where each wheel is controlled by two motors to drive and steer. The omnidirectional mobile robot that takes the spherical wheel as the travelling mechanism is also widely investigated [19] and later generations are also improved according to its shortcomings [20]. Artificial intelligence technology is still developing rapidly, and the demand for mobile robots in various fields is continuously increasing. Therefore, the research of mobile robot has a great development prospect.

Although the Mecanum wheel is used relatively widely in the field of mobile robots, it's disadvantages are also obvious. The distinct characteristic of the Mecanum wheel is that the rollers are evenly distributed around the rim [21], which causes inevitably vibration and slipping in motion [22]. While the each wheel of ordinary wheeled omnidirectional mobile robots generally manipulated by at least two motors, which not only wastes resources, but also increases the difficulty of control [23], [1]. There is a study indicates that the motion of different driving wheels is controlled separately [2]. And most existing mobile robots are redundant drivers [24]. This paper emphasizes an under-actuated omnidirectional mobile robot that each wheel only need to be equipped with one motor to complete omnidirectional motion, and this robot can steer flexibly even in a narrow space with the unchanged attitude during the movement compared with other mobile robots.

The remainder of the paper is arranged as follows: Section II mainly introduces the analysis of the under-actuated omnidirectional mobile robot. The comparison between the simulation results and experimental results under different environments and different trajectories is presented in Section III. The final part gives a summary for the paper.

II. ANALYSIS OF UNDER-ACTUATED OMNIDIRECTIONAL MOBILE ROBOT

A. SYSTEM ANALYSIS

This subsection contains two parts, the first introduces the components of this omnidirectional mobile robot and the second part mainly includes the control method of this system. A significant concept of under-actuated also is put forward in this segment.

1) HARDWARE STRUCTURAL SYSTEM ANALYSIS

The integral model diagram and the splitting diagram of the under-actuated omnidirectional mobile robot investigated in this paper is shown in Fig. 1. The robot is mainly composed of front body, rear body, parallelogram connecting rod, vertical rotation axis, and four wheels. Considering the limitations of the Mecanum wheel to the use of the ground, this paper regards the ordinary wheel as the travelling mechanism, the wheels deviate from the vertical rotation axis and a pair of wheels is mounted on the inside of the vertical rotation axis and the other pair is mounted on the outside. Refer to previous studies [17], how to ensure smooth motion on uneven ground is also considered. In order to keep the force balance of the robot even on the rugged ground, its body is divided into front body and rear body, where the front body is a fixed part and the rear body is a part that can swing along the vertical direction (the pendulum angle is approximately between $-20°$ and $20°$), both of them are attached via a smooth connecting rod. The parallelogram connecting rod and the vertical rotation aixs are connected by a crank. We add a spring as the buffer between parallelogram connecting rod and crank, which not only avoids collision between them,

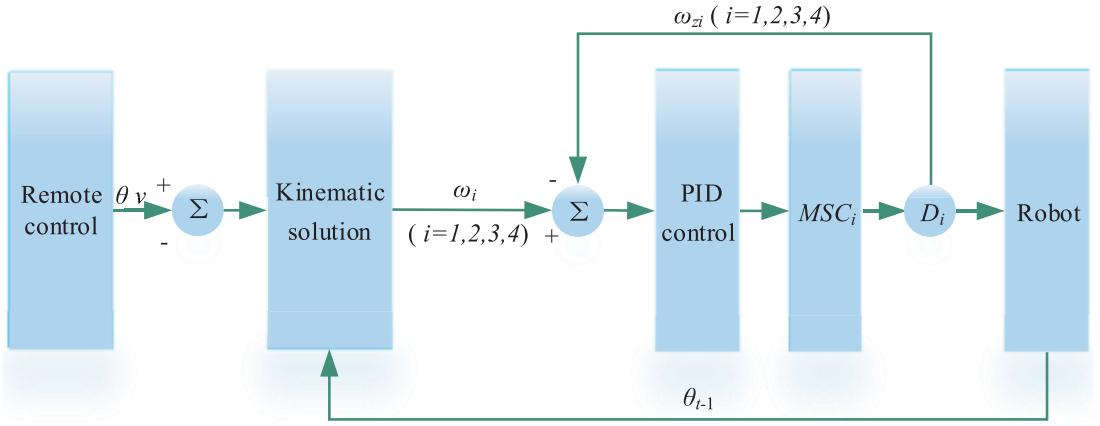

FIGURE 2. The flow chart of control program execution. It shows the process of the data interaction between the remote control and the robot.

but also provides a degree of freedom along the vertical direction, ensuring that the additional resistance caused by other assembly errors can be offset to some extent.

What is worth emphasizing is the parallelogram connecting rod attached to the robot body, which is drawn in Fig. 1. It connects the four vertical rotation axis to enable the four wheels to generate the same steering angle around the corresponding vertical rotation axis. By adjusting the relationship of speed (the difference of direction) between wheels, the robot can move in all directions. And the attitude of the robot keeps constant during the movement, which will be illustrated in the next part.

In view of the structure designed in this paper, each set of wheel has two degrees of freedom. One is the rotation of the wheel itself (we can regard this motion as the translation of the vertical rotation axis), the other is the rotation of wheel around the vertical rotation axis. As compared to the traditional structure, the structure proposed in this paper only need one motor to drive the rotation of each wheel, as can be seen from Fig. 1. The rotation around the vertical rotation axis is free without any driver. That is to say, this structure realizes the rotation and translation of the vertical rotation axis using one motor.

2) CONTROL SYSTEM ANALYSIS

In this paper, Cortex-M4 is selected as the robot control platform and uses remote controller to transmit command. The real-time manipulation of the mobile robot is realized by the two black rockers of the remote controller, the left one controls the straight walking, and the right one controls the steering of the robot. While the motions in accordance with the preset trajectory (include square trajectory and serpentine trajectory) are controlled by the upper switches. We select angle sensor as feedback angle receiving device.

The implementation of the control system can be expressed as follows: The angle value from remote controller is transferred to the control board. Then the main control board acquires the external signal to execute the kinematics analysis to obtain the motion signal of each wheel, which will be further figured out by PID control. Finally the output that can drive the movement of the wheel will be obtained and transmitted to the corresponding motor through Brushless DC Motor Speed Controller(MSC), so as to realize the control of the robot. As for the actual steering angle can be detected by the angle sensor. The flow chart of control program execution is presented as Fig. 2, where D_i represents motor, $i = 1,2,3,4$.

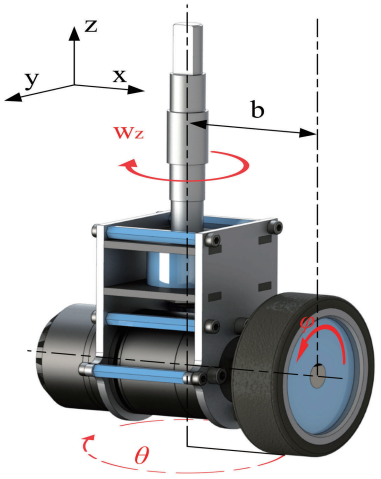

FIGURE 3. Rotation of single wheel. We use it as a simplified model to analyze the kinetics analysis of robot.

B. KINETIC ANALYSIS

According to the existing studies [25], [26], it is an effective way to explain the rationality of the design by analyzing the dynamics and kinematics of the model. So, in order to verify the superiority of the steering method proposed in this paper, this segment describes the force of the parallelogram linkage under different motion conditions due to the motion coupling of four wheels.

Assume that each wheel keeps balance on the ground and does pure rolling motion without skidding, and the friction of the bearing on the vertical rotation axis is omitted. For convenience, as shown in Fig. 3, the rotation of one wheel

around the vertical rotation axis is extracted from the overall motion. The momentum moment of the wheel around the vertical rotation axis is:

$$L_z = J_z \omega_z \tag{1}$$

where, J_z is the wheel's moment of inertia around vertical rotation axis, ω_z is the angular velocity of particles on vertical rotation axis due to the turning of wheels. To the best of our knowledge, the expression for the torque M_z can be given below:

$$\frac{d}{dt} L_z = M_z \tag{2}$$

By calculating the first derivative of (1) and combined with (2), the following equation can be obtained:

$$M_z = J_z \frac{d\omega_z}{dt} \tag{3}$$

We use M_i to express the torque exerts on different vertical rotation axis and it can be proposed as follows (i = 1,2,3,4. The meaning of i that occurs below is the same):

$$M_i = J_z \frac{d\omega_{zi}}{dt} \tag{4}$$

Then, according to the knowledge of physics that we learned before, (4) is also can be extended as follows:

$$M_i = J_z \frac{d\omega_{zi}}{dt} = F_{fi} b - F_{li} d \tag{5}$$

where F_{fi} is the total force acting on the wheels. Because that the vertical rotation axis is parallel to the direction of the support force from ground, we just take the friction that generated during movement and the motor driving force into account. F_{li} (i = 1,2,3,4) is the constraining force, from the parallelogram connecting rod, which exerts on the four cranks. ω_{zi} shows the angular velocity of different vertical rotation axis. b is the cantilever length between the center of the wheel to the vertical rotation axis. d is the length of the crank. In order to illustrate some characteristics of the robot in motion, the following two kinds movements are analyzed. 1. In situ rotation: Take the clockwise rotation of the wheel around the vertical rotation axis as an example, the state of the wheels at a certain moment in the steering process is shown in Fig. 4. What can be analyzed is that the force acting on different wheels are in opposite directions, which causes the speed difference between wheels (the direction is different). That is $v_1 = v_3 = -v_2 = -v_4$. So the torque generated by the force which acts on the wheel is equal when the wheels turn. Immediately following this, we take the force acting on the parallelogram connecting rod to analyze. The friction is ignored, so here we just consider the force from the crank to analyze the effect on motion. We can conclude according to (5) that the total torque around the vertical rotation axis depends on F_{fi} and F_{li}. Obviously, the conclusion obtained through the analysis of Fig. 4 is the relationship of force between wheels is $F_{f1} = -F_{f2} = F_{f3} = -F_{f4}$. On this occasion, in order to satisfy the relationship $M_1 = M_2 = M_3 = M_4$ to accomplish its clockwise rotation, the following

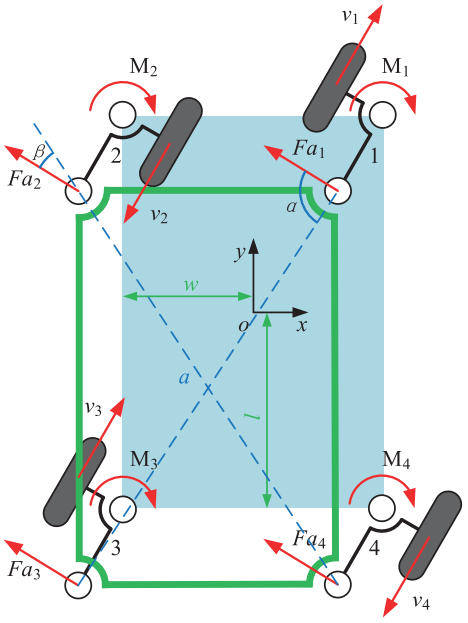

FIGURE 4. The state of the robot at a certain moment when robot is in situ rotation, it includes the stress condition of wheels and parallelogram connecting rod.

relationship must be satisfied: $F_{l1} = F_{l2} = F_{l3} = F_{l4}$. Actually, the specific orientation of force has inessential effect as long as the directions of them stay the same as well as perpendicular to the crank. Given that the conclusion is reflected through the analysis of parallelogram connecting rod, we set the force of the four cranks to a parallelogram connecting rod is F_{ai} and it satisfies the expression of $F_{ai} = -F_{li}$. In that way, the resultant force on centroid of parallelogram connecting rod can be calculated as:

$$F_a = \sum F_{ai} \tag{6}$$

A possible situation as shown Fig. 4 is selected to perform next analysis. What can be obtained is: $F_a \neq 0$, and its direction is in tune with the direction of F_{ai}. Since the cranks are always parallel to the wheels, furthermore, the direction of F_a will change along with the orientation change of wheels, which causes the parallelogram connecting rod to translate in the x-y plane. In addition, The principal moment relative to the centroid of the parallelogram connecting rod M_c can be expressed as below:

$$M_c = F_{a1} \frac{a}{2} \sin\alpha - F_{a3} \frac{a}{2} \sin\alpha + F_{a2} \frac{a}{2} \sin\beta - F_{a4} \frac{a}{2} \sin\beta \tag{7}$$

where a is the diagonal length, α is the angle between F_{a1} and diagonal, β is the angle between F_{a2} and diagonal. The result can be calculated in the motion state of Fig. 4 is $M_c = 0$, and it keeps zero as long as the wheel is balanced. That is to say, the parallelogram connecting rod will not rotate around the x or y axis. The above derivation shows that the parallelogram connecting rod will just translate when the wheels steer, without turning over. It is indirectly illustrated

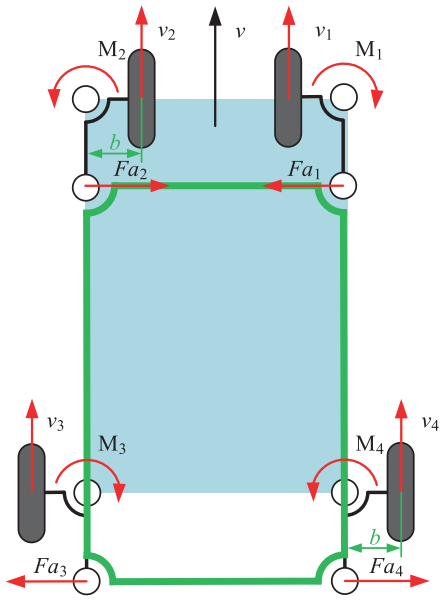

FIGURE 5. The state of the robot at a certain moment when robot goes straightly, the stress condition of wheels and parallelogram connecting rod also can be seen in this simplified diagram.

that the orientation of four links of it remains unchanged. While the four links of robot's body are always parallel to the parallelogram connecting rod's respectively. What ultimately is the attitude of the robot keep consistent during the steering. 2. Walk straightly: When the wheels go straightly, the speed of wheels and torques around the vertical rotation axis in this motion is showed in Fig. 5. We can analyze that the wheels are equal in speed and the torque around the vertical rotation axis due to the rotation of wheels has opposite direction between each two neighboring wheels. Under the circumstances, in order to tally with the actual movement, e.g. the wheels are not allowed to turn, following relationship must be satisfied: $M_1 = M_2 = M_3 = M_4 = 0$. So the direction of F_{ai} is just the case in Fig. 5 and the following equation can be seen:

$$F_{a1} = F_{a3} = -F_{a2} = -F_{a4} \tag{8}$$

What Fig. 5 presents is the force acting on parallelogram connecting rod from cranks when the mobile robot goes straightly. The analysis is the same as in the previous case. The result that by substituting (8) into (6) is $F_a = 0$. Referring to (7), what can be obtained is $M_c = 0$. In this case, the parallelogram connecting rod will neither translate nor overturn, which also indirectly proves the attitude of the robot body keeps unchanged.

By analyzing the above two motions of the robot, it can be seen that the speed difference exits between wheels when the wheels steer and the velocity of wheels are equal when it goes straightly. After theoretical analysis, the result is that the rotation of the wheel around the vertical rotation axis ultimately can only generates a resultant force which acts on the parallelogram connecting rod to make the parallelogram connecting rod to translate, which will not affect the direction of the robot body during the exercise. While the rotation around the vertical rotation axis does not require a motor to drive.

C. KINEMATIC ANALYSIS

It's worth mentioning that the robot is completely omnidirectional, in addition to the above analysis of the two kinds of the ability to move, it also has the ability to turn, as shown in Fig. 5, when $v_1 = v_4 > v_2 = v_3$, similar to the above analysis, we can get $F_a = 0, M_c = 0$, in this case, because of the speed difference between the left and right wheels, the robot will deflection.

But we consider that there are many advantages to using in a particular situation (such as movement in a narrow space) when the robot keep constant attitude. And then we consider the kinematics analysis of the robot with the constant attitude.

1) STEERING ANGLE ANALYSIS OF WHEEL

According to the analysis in the previous section, each wheel will rotate around its corresponding vertical rotation axis when steering. The relationship between the steering angle of wheel and the corresponding arc length is presented as below:

$$L = b*\theta \tag{9}$$

where, θ is the steering angle along the ground when the wheel rolls from one place to another, which will be feedback by angle sensor. And we use $\theta = \theta_t - \theta_{t-1}$ to represent it (Let's stipulate that the motion starts at time zero), θ_{t-1} represents the initial angle of wheel at the start of each motion, θ_t represents the angle value at time t. L is the arc length corresponding to θ. For convenience, it is assumed that the initial steering angle of the wheel is $\theta_{t-1} = 0$. And the relevant analysis is conducted on the assumption that wheel does not slipping, so the path S that the wheel rolls over can be calculated as:

$$S = r*\varphi \tag{10}$$

$$S = L \tag{11}$$

where φ is the rotation angle of the wheel around the x-axis direction, as presented in Fig. 3. At which the wheel rolls purely along the ground and the angle is reflected by the motor. r is the radius of wheel. Through the derivation of the (9), (10) and (11), the following equation can be obtained:

$$\varphi = \frac{b}{r}\theta \tag{12}$$

By calculating the first derivative of the (12), the expression for the angular velocity of the wheel as it rolls purely along the ground ω_c can be presented as below:

$$\omega_c = \frac{b}{r}\frac{d\theta}{dt} \tag{13}$$

2) KINEMATIC SOLUTION

In consideration of the robot's motion just in two-dimensional space, the two-dimensional coordinate systems are set up as shown in Fig. 6, the world coordinate system{**A**}, robot

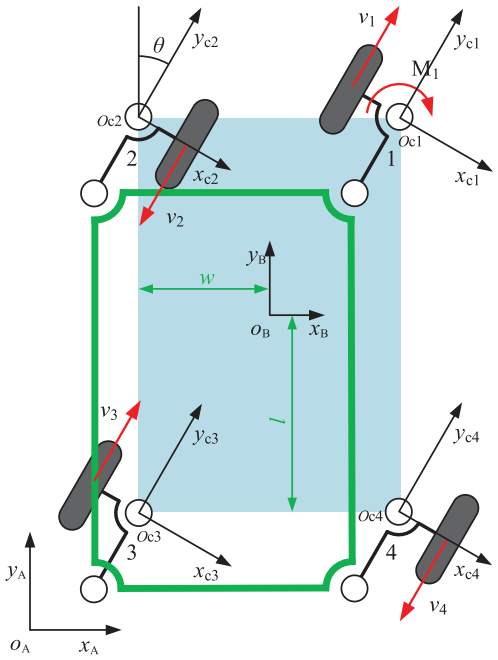

FIGURE 6. The world coordinate system, robot coordinate system and wheel coordinate system.

coordinate system{**B**} and wheel coordinate system $\{\mathbf{C}_i\}$ $(i = 1,2,3,4)$ are established respectively. Where, the origin of the robot coordinate system $\mathbf{O}_B$ coincides with the centroid of the robot, the positive direction of the y-axis is along the direction of the robot body, the origin of the wheel coordinate system $\mathbf{O}_{ci}$ coincides with the intersection of the motor shaft and the vertical axis of rotation. The position of wheel 1 in the wheel coordinate system $\{\mathbf{C}_1\}$ is ${}^{c1}\mathbf{p}_1 = [-b, 0]^T$, the position of wheel 2 in the wheel coordinate system ${}^{c2}\mathbf{p}_2 = [b, 0]^T$, the position of wheel 3 in the wheel coordinate system $\{C_3\}$ is ${}^{c3}\mathbf{p}_3 = [-b, 0]^T$, the position of wheel 4 in the wheel coordinate system $\{C_4\}$ is ${}^{c4}\mathbf{p}_4 = [b, 0]^T$. And the coordinates of each wheel in its own coordinate system always stay the same. In this paper, it is stipulated that the rotation angle of the wheel coordinate system around the z-axis takes the positive half axis of the y-axis of the robot coordinate system as the starting point, and the clockwise direction is positive. The position of the origin of the coordinate system of wheel 1, wheel 2, wheel 3 and wheel 4 in the robot coordinate system {**B**} is respectively expressed as ${}^{B}\mathbf{p}_{c1} = [w, l]^T$, ${}^{B}\mathbf{p}_{c2} = [-w, l]^T$, ${}^{B}\mathbf{p}_{c3} = [-w, -l]^T$, ${}^{B}\mathbf{p}_{c4} = [w, -l]^T$. According to the homogeneous coordinate transformation, the position of each wheel in the robot coordinate system {**B**} is expressed:

$$ {}^{B}\mathbf{p}_i = {}^{B}_{ci}\mathbf{R}(\theta)\,{}^{ci}\mathbf{p}_i + {}^{B}\mathbf{p}_{ci} \tag{14} $$

${}^{B}_{ci}\mathbf{R}(\theta)$ is a two-dimensional rotation matrix, the other presentation of θ in here is the rotation angle of $\{\mathbf{C}_i\}$ relative to {**B**}, but is equal to the presentation as before. The equation can be shown as follows:

$$ {}^{B}_{ci}\mathbf{R}(\theta) = \begin{bmatrix} \cos\theta & \sin\theta \\ -\sin\theta & \cos\theta \end{bmatrix} \tag{15} $$

According to the above analysis, the attitude of the robot remains unchanged during the movement. Therefore, the robot coordinate system {**B**} only translate with respect to the world coordinate system {**A**} without rotation. When the robot is in a certain state, the position of the robot in the world coordinate system can be expressed as ${}^{A}\mathbf{p}_B = [x, y]^T$. And the position of each wheel in the world coordinate system can be expressed as:

$$ {}^{A}\mathbf{p}_i = {}^{A}\mathbf{p}_B + {}^{A}_{B}\mathbf{R}(\gamma)\,{}^{B}\mathbf{p}_i \tag{16} $$

where γ is the rotation angle of the robot coordinate system relative to the world coordinate system and $\gamma = 0$. According to (14), (15) and (16), the following equation can be presented as:

$$ {}^{A}\mathbf{p}_i = {}^{A}\mathbf{p}_B + {}^{A}_{B}\mathbf{R}(\gamma)\,{}^{B}_{ci}\mathbf{R}(\theta)\,{}^{ci}\mathbf{p}_i + {}^{A}_{B}R(\gamma)\,{}^{B}\mathbf{p}_{ci} \tag{17} $$

By calculating the first derivative of (17), the speed of wheels in the world coordinate system can be obtained as $\left({}^{A}\mathbf{p}_i\right)'$. The specific relationship is as follows:

$$ v_i = {}^{A}\mathbf{p}_B{}' + {}^{A}_{B}\mathbf{R}(\gamma)\,{}^{B}_{ci}\mathbf{R}(\theta)'\,{}^{ci}\mathbf{p}_i \tag{18} $$

And ${}^{A}\mathbf{p}_B{}'$ is the velocity of the robot relative to the world coordinate system. It can be presented as below:

$$ {}^{A}\mathbf{p}_B{}' = \begin{bmatrix} x' \\ y' \end{bmatrix} = \begin{bmatrix} v\sin\theta \\ v\cos\theta \end{bmatrix} \tag{19} $$

where v is the moving speed of the robot, whose direction is parallel to the y-axis of the wheel coordinate system, and this value is obtained by coupling the speeds of the motors. The speed of each wheel can be calculated according to (14), (17) and (18) (θ is a vector), the form is:

$$ v_1 = v_3 = v + b\frac{d\theta}{dt} \tag{20} $$

$$ v_2 = v_4 = v - b\frac{d\theta}{dt} \tag{21} $$

Considering that $v_i = \omega_i r$, the angle velocity of each wheel is shown as follows:

$$ \omega_1 = \omega_3 = \frac{v}{r} + \frac{b}{r}\frac{d\theta}{dt}, \quad \omega_2 = \omega_4 = \frac{v}{r} - \frac{b}{r}\frac{d\theta}{dt} \tag{22} $$

The basis of the above discussion is that we assume the initial steering angle of the wheel is $\theta_{t-1} = 0$. Actually, the actual initial angle position of the wheel is different when different steering movement is executed. Applying above conclusions to general case, that is to say $\theta = \theta_t - \theta_{t-1}$ and $\theta_{t-1} \neq 0$. We can obtain the expression of angular velocity of wheel is:

$$ \begin{bmatrix} \omega_1 \\ \omega_2 \\ \omega_3 \\ \omega_4 \end{bmatrix} = \frac{1}{r}\begin{bmatrix} 1 & b \\ 1 & -b \\ 1 & b \\ 1 & -b \end{bmatrix}\begin{bmatrix} v \\ \frac{d\theta}{dt} \end{bmatrix} \tag{23} $$

What can be drawn from this section is the speed of the wheel is determined by v and θ. Furthermore, the movement status of the wheel is determined by the moving speed of the robot and the speed attached to a wheel due to the rotation around the vertical rotation axis.

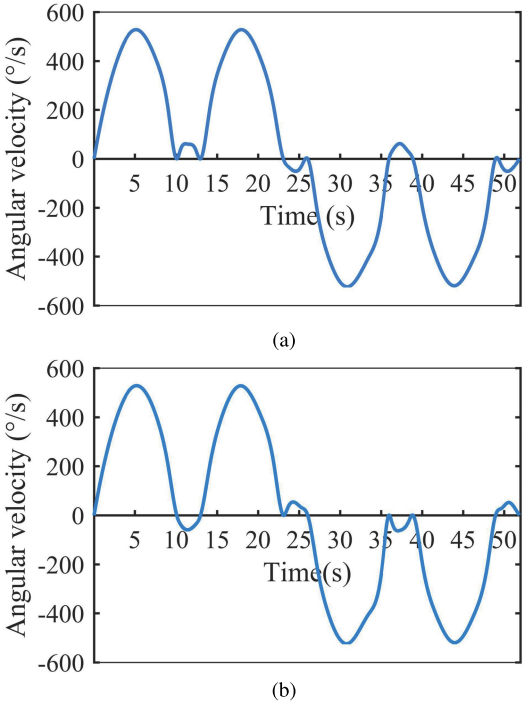

FIGURE 7. The angular velocity of the wheels, (a)Lower left wheel. (b)Upper left wheel.

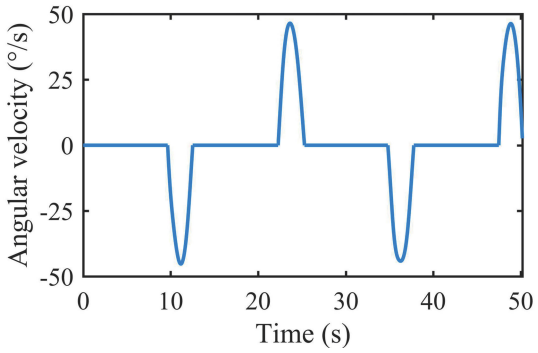

FIGURE 8. The angular velocity change of the rotation axis.

III. SIMULATION AND EXPERIMENTAL RESULTS ANALYSIS OF UNDER-ACTUATED OMNIDIRECTIONAL MOBILE ROBOT

A. THE ANALYSIS OF SIMULATION AND EXPERIMENTAL RESULTS OF DIFFERENT MOTION TRAJECTORIES

The motion simulation in this paper is completed by using the plug-in of Solidworks 2014. By switching the upper switch of the remote controller, we select the preset square trajectory and serpentine trajectory for simulation and experiment, and then compared the simulation results with the experimental results.

1) SIMULATION AND EXPERIMENTAL RESULTS ANALYSIS OF SQUARE TRAJECTORY

According to the previous analysis, the conclusion is that when the speed of the four wheels is consistent, the mobile robot will walk straightly, and when the speed difference occurs, the moving direction of wheel will change. Before making prototype, we simulate the square trajectory in the simulation software. Finally the angular velocity of the lower left wheel and the upper left wheel is shown in Fig. 7(a) and Fig. 7(b), the angular velocity of the upper right wheel keeps consistence with the lower left wheel, while the angular velocity of the upper left wheel keeps consistence with the lower right wheel. Fig. 8 presents the angular velocity of one of the rotation axis. We can see that when the speed between the lower left wheel and the upper left wheel is the same, the angular velocity of the rotation axis is zero which represents the robot is going straightly. When there is a difference in the speed between wheels, the angular velocity of the vertical rotation axis varies with some regularity. During this time the robot's wheel is steering and the direction of rotation is partial to the larger speed.

After the prototype, shown in Fig. 9, is made successfully. We control the robot to walk following the square trajectory by coding the control command to the control board. The trajectory is drawn by a marker pen attached to the end of the robot. Fig. 9 shows the status of the robot at each right angle when moving along the square trajectory, in which (a) presents the initial state of the robot, and it can be seen that the wheel is placed toward the longitudinal direction. After arriving at the first right angle along the first brim, the state of wheels is shown in the (b), in which we can see that the wheels turn clockwise 90° relative to the initial position. (c) and (d) illustrate the state of wheels at the second right angle and the third right angle, respectively. It is worth stressing that when the robot wants to change its moving direction, all that changes is the turning of wheels, while the attitude of body is unchanged. We take floor seam as a reference, the robot's walking trajectory is parallel to floor seam and the overall trajectory is indeed square, which is consistent with the simulation results. This experiment provides a favorable evidence for the correctness of the above theoretical derivation. Fig. 10 includes the zigzag curve of the input angle from remote controller and the actual trajectory angle which is fed back by the angel sensor in a square motion cycle. The four oblique lines are the angle change process of the robot during it steering at each right angle respectively. While the four lines parallel to the horizontal axis are the angle change of wheels during the straight walking. What can be seen from the Fig. 10 is that the angle changes from 0° to 90°, that is to say, the changing process of angle completely conforms to the change rule of the robot moving along the square trajectory. This experiment verifies the feasibility and correctness of the structure, which also indirectly proves the rationality of the previous theoretical analysis. On the problem that the response curves do not coincide during the turning, it is possible to be caused by unreasonable assembly of the structure after analysis. But it doesn't affect the overall performance.

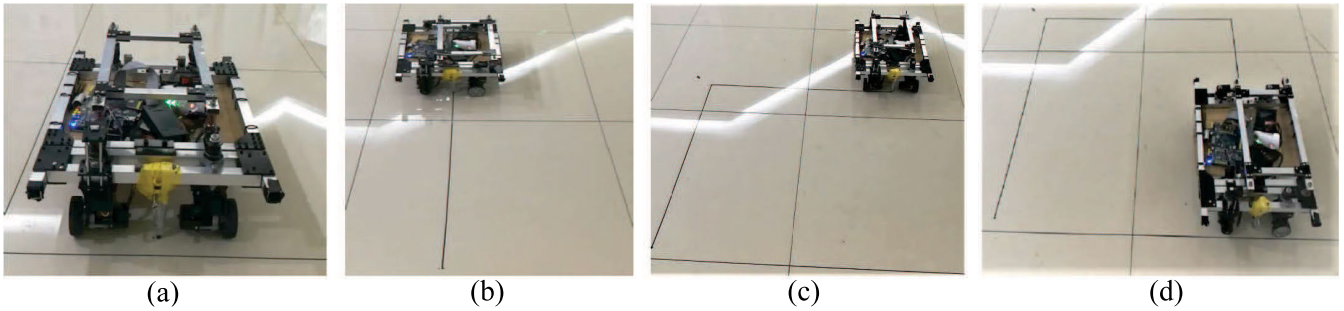

FIGURE 9. The status of the robot at each right angle.

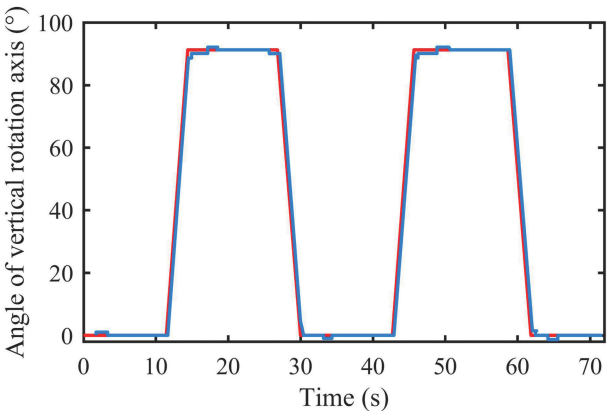

FIGURE 10. The angle change during a period of a square trajectory, the red line represents the set value of remote control, the blue line represents the feedback value of sensor.

2) SIMULATED AND EXPERIMENTAL RESULTS ANALYSIS OF SERPENTINE TRAJECTORY

By setting the steering angle of the wheel changes within $-90°$ to $90°$, the angular velocity of the wheel's vertical rotation axis is sinusoidally changed. We set the magnitude of robot's moving speed v as a certain value, and v determines the amplitude of the curve. Following data curves are obtained from the simulation of serpentine trajectory. We can see from Fig. 11, the speed of the wheels on the two diagonals always changes in an opposite trend. Therefore, the speed difference between wheels constantly exits, which makes the wheels keep turning according to a certain rule. As expected, the angular velocity of the rotation axis of the wheel is indeed changing according to the sine curve. When the wheel speed difference reaches the maximum, the angular velocity of the vertical rotation axis also reaches the maximum.

The control program is also written to control the robot to walk following the serpentine trajectory. When the serpentine experiment is performed, we set the change range of steering angle keeps consistent with the simulation. The initial angle position of robot is selected as $\theta_{t-1} = 0°$. In Fig. 12, (a) shows the state of wheels when turning counterclockwise of 90° respective to the initial position. And (b) shows the state of wheels after turning counterclockwise of 180° respective to the initial position. The state of wheels after turning clockwise of 180° respective to (b) is shown in (c), while (d) shows the state of wheels after turning counterclockwise of 90° respective to (c). We use gyroscope to verify if the attitude of the robot keeps constant during the movement. The gyroscope is anchored on the body of the robot. The difference between the gyroscope's value during the movement and the initial position represents the angle change of the robot body. The comparison results is shown in the Fig. 13. It is easy to find that the error between them is about -0.3 degree to 0.3 degree. The error is too small to ignore. So we can regard that the attitude of the robot

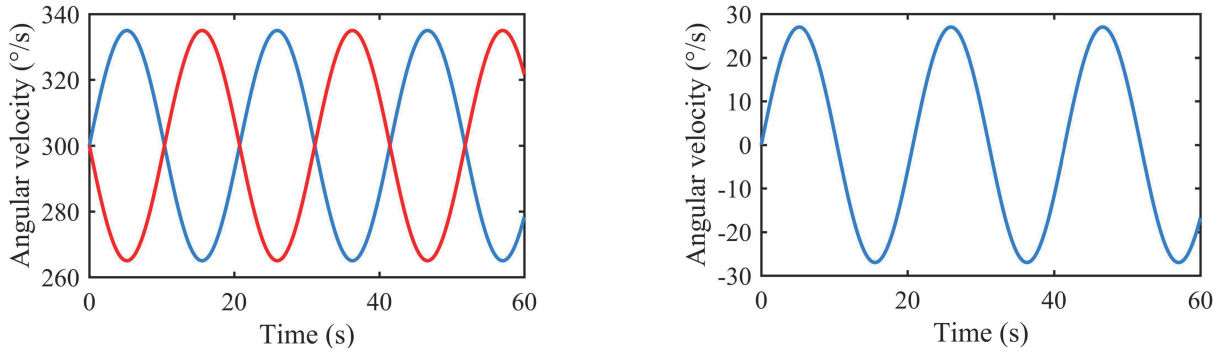

FIGURE 11. The change of the angular velocity over the movement, (left) represents the comparison between Lower left wheel and upper left wheel, (right) represents angular velocity of the vertical rotation axis.

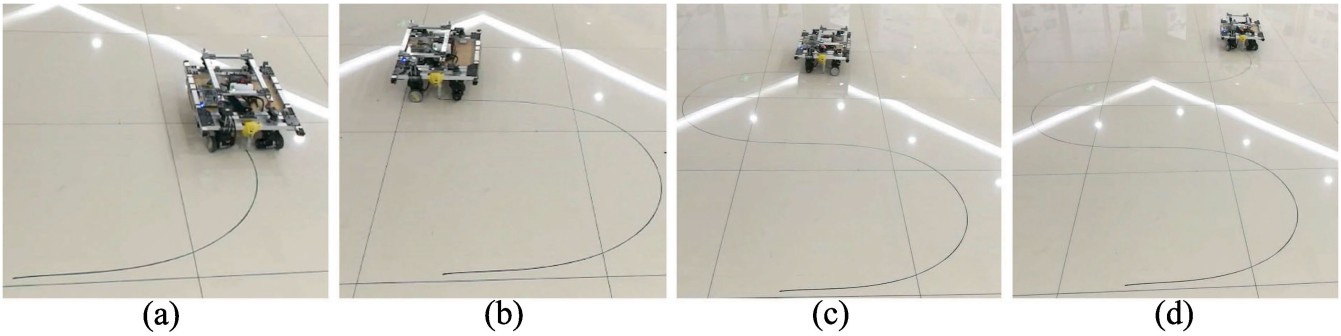

FIGURE 12. Serpentine trajectory partial state point.

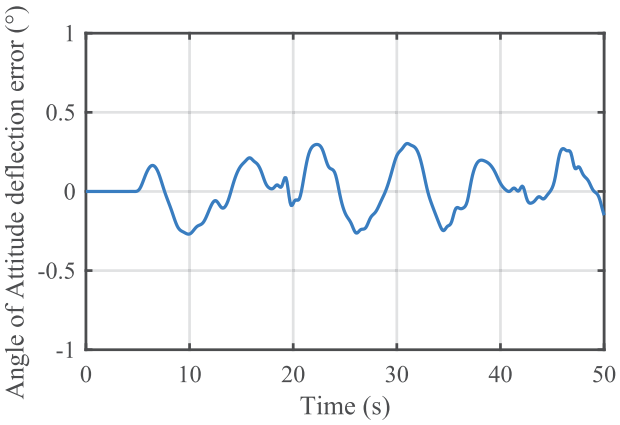

FIGURE 13. The difference between the gyroscope's value during the movement and the initial position represents the angle change of the robot body.

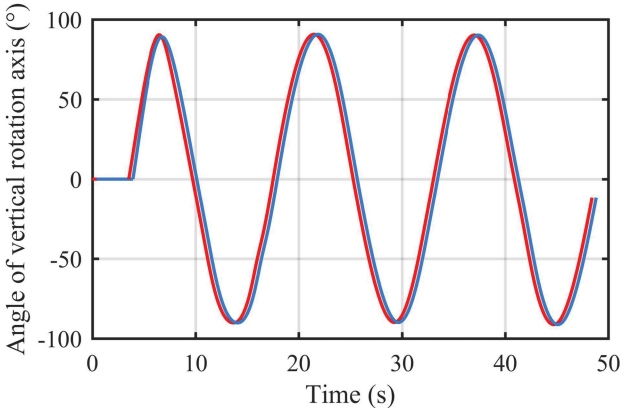

FIGURE 14. The angle change during a period of a serpentine trajectory, the red line represents the set value of remote control, the blue line represents the feedback value of sensor.

still keep constant during the movement. When the robot moves in a serpentine trajectory, the relationship between time and angle is shown as Fig. 14. The two curves are also respectively present the angle change transmitted by the remote controller and fed back by the angle sensor, and they basically overlap. In summary, the consistent conclusion with the square trajectory experiment is got.

Both of above experiments provide an excellent evidence that the mobile robot can realize omnidirectional movement by the speed coupling via parallelogram connecting rod with

FIGURE 15. The experiment on the potholed road.

FIGURE 16. The experiment on the gravel road.

the least number of motors. For a single set of wheel, the number of freedom is greater than the number of motor, so it can be regarded that it is bounded with non-holonomic constraints during the movement of robot [3], [27], [28]. In addition, it is also verified that the speed of the wheels between the two diagonals is opposite when steering and the speed of four wheels is same when going straightly. The characteristic of the robot that the attitude remains unchanged during the movement is also well reflected.

B. EXPERIMENTS IN VARIOUS EXPERIMENTAL ENVIRONMENTS

In order to verify whether the under-actuated omnidirectional mobile robot designed in this paper has good adaptability and stability, some rough and harsh outdoor fields are selected to test. Fig. 15 shows the experiment on the potholed road and Fig. 16 shows the experiment on the gravel road. We just simply try to verify its adaptability, so no data is recorded.

In the above two experimental environments, remote controller is used to drive the robot performs go straightly, steer and then translate motion respectively. The results show that the under-actuated omnidirectional mobile robot can successfully pass through the above three ground environments and

flexible steering also can be achieved. The tests prove that the under-actuated omnidirectional mobile robot has strong stability and good adaptability to the ground environment.

IV. CONCLUSION

Compared with the traditional mobile robot, this paper designs an under-actuated omnidirectional mobile robot with low power consumption and small usage space. After theoretical and experimental analysis, we have verified that we regard the parallelogram connecting rod as the speed coupling system which is designed in this paper enable the wheels to achieve omnidirectional movement because of the change in the relationship of speeds between wheels. That is to say, we have successfully implemented one motor to control the motion of two degrees of freedom of each wheel. The design of the structure also makes the robot's attitude remain unchanged during the movement, which make it turn flexibly in a small radius even in a narrow space. The square trajectory and serpentine trajectory are selected for motion simulation and physical test, the roughly same trajectory and velocity curves are obtained by comparing both of them, and the curve of attitude angle change in motion process is also obtained through experiment. The results verify the rationality of the overall design scheme. In order to verify the adaptability of the mobile robot to the environment, controlling the robot performs the walking and steering actions in two harsh environments, namely, potholed road and gravel road. The outcomes prove that the under-actuated omnidirectional mobile robot can smoothly go through the above two ground environments, possesses good adaptability to the ground environment.

REFERENCES

[1] G. Ishigami, K. Iagnemma, J. Overholt, and G. Hudas, "Design, development, and mobility evaluation of an omnidirectional mobile robot for rough terrain," *J. Field Robot.*, vol. 32, no. 6, pp. 880–896, Sep. 2015. doi: 10.1002/rob.21557.

[2] S. Sakai, H. Sado, and Y. Hori, "Motion control in an electric vehicle with four independently driven in-wheel motors," *IEEE/ASME Trans Mechatronics*, vol. 4, no. 1, pp. 9–16, Mar. 1999. doi: 10.1109/3516.752079.

[3] T. Jacobs, M. Hesse, and A. Verl, "Evaluation of wheel mechanisms for omnidirectional robot undercarriages," in *Proc. ISR/Robotik 41st Int. Symp. Robot.*, Jun. 2014, pp. 1–7.

[4] V. A. Joshi, R. N. Banavar, and R. Hippalgaonkar, "Design and analysis of a spherical mobile robot," *Mech. Mach. Theory*, vol. 45, no. 2, pp. 130–136, Feb. 2010. doi: 10.1016/j.mechmachtheory.2009.04.003.

[5] N. J. Nilsson, "A mobile automaton: An application of artificial intelligence techniques," in *Proc. 1st Intl. Joint Conf. Artif. Intell. (IJCAI).*, Seattle, WA, USA, Jan. 1969, pp. 509–520.

[6] P. Muir and C. Neuman, "Kinematic modeling for feedback control of an omnidirectional wheeled mobile robot," in *Proc. IEEE Intl. Conf. Robot. Automat.*, Mar./Apr. 1987, pp. 1772–1778.

[7] J. Agulló, S. Cardona, and J. Vivancos, "Kinematics of vehicles with directional sliding wheelsCinematique des vehicules a roues de glissement directionnel," *Mechanism Mach. Theory*, vol. 22, no. 4, pp. 295–301, 1987. doi: 10.1016/0094-114x(87)90018-8.

[8] J. E. M. Salih, M. J. M. Rizon, S. Yaacob, A. Adom, and M. R. Mamat, "Designing omni-directional mobile robot with mecanum wheel," *Amer. J. Appl. Sci.*, vol. 3, no. 5, pp. 1831–1835, May 2006.

[9] L. D. Zhang and C. J. Zhou, "Kuka youBot arm shortest path planning based on geodesics," in *Proc. IEEE Int. Conf. Robot. Biomimetics*, Dec. 2013, pp. 2317–2321.

[10] R. Bischoff, U. Huggenberger, and E. Prassler, "KUKA youBot—A mobile manipulator for research and education," in *Proc. IEEE Int. Conf. Robot. Automat.*, May 2011, pp. 1–4.

[11] Z. Schnepp, "Giant robotic vehicle moves aircraft parts (NEWS & analysis)," *Prof. Eng.*, vol. 29, pp. 6–7, Aug. 2016.

[12] A. Gfrerrer, "Geometry and kinematics of the Mecanum wheel," *Comput. Aided Geometric Des.*, vol. 25, no. 9, pp. 784–791, Dec. 2008. doi: 10.1016/j.cagd.2008.07.008.

[13] G. Runge, G. Borcher, P. Henke, and A. Raatz, "Design and testing of a 2-DOF ball drive," *J. Intell. Robotic Syst.*, vol. 81, no. 2, pp. 195–213, Feb. 2016. doi: 10.1007/s10846-015-0247-6.

[14] Y. Zhao and S. L. BeMent, "Kinematics, dynamics and control of wheeled mobile robots," in *Proc. IEEE Int. Conf. Robot. Automat.*, May 1992, pp. 91–96.

[15] J.-B. Song and K.-S. Byun, "Design and control of a four-wheeled omnidirectional mobile robot with steerable omnidirectional wheels," *J. Robotic Syst.*, vol. 21, no. 4, pp. 193–208, Apr. 2010. doi: 10.1002/rob.20009.

[16] G. Campion, G. Bastin, and B. D'Andrea-Novel, "Structural properties and classification on kinematic and dynamic models of wheeled mobile robots," *Nelineinaya Dinamika*, vol. 7, no. 4, pp. 733–769, 2011. doi: 10.1109/70.481750.

[17] M. Udengaard and K. Iagnemma, "Kinematic analysis and control of an omnidirectional mobile robot in rough terrain," in *Proc. IEEE/RSJ Int. Conf. Intell. Robots Syst.*, Oct./Dec. 2009, pp. 795–800.

[18] B. Dumitrascu, A. Filipescu, A. Radaschin, and E. Minca, "Discrete-time sliding mode control of wheeled mobile robots," in *Proc. 8th Asian Control Conf.*, May 2011, pp. 771–776.

[19] S. Ma, C. Ren, and C. Ye, "An omnidirectional mobile robot: Concept and analysis," in *Proc. IEEE Int. Conf. Robot. Biomimetics*, Dec. 2012, pp. 920–925.

[20] Y.-C. Lee, D. V. Lee, J. H. Chung, and S. A. Velinsky, "Control of a redundant, reconfigurable ball wheel drive mechanism for an omnidirectional mobile platform," *Robotica*, vol. 25, no. 4, pp. 385–395, Jul. 2007. doi: 10.1017/S0263574706003158.

[21] I. Doroftei, "Conceptual design of an omni-directional mobile robot," in *Proc. SYROM*, Nov. 2009, pp. 115–127.

[22] C. M. Gosselin and J. Angeles, "Singularity analysis of closed-loop kinematic chains," *IEEE Trans. Robot. Autom.*, vol. 6, no. 3, pp. 281–290, Jun. 1990. doi: 10.1109/70.56660.

[23] G. Ishigami, E. Pineda, J. Overholt, G. Hudas, and K. Iagnemma, "Performance analysis and odometry improvement of an omnidirectional mobile robot for outdoor terrain," in *Proc. IEEE/RSJ Int. Conf. Intell. Robots Syst.*, San Francisco, CA, USA, Sep. 2011, pp. 4091–4096.

[24] K.-S. Byun, S.-J. Kim, and J.-B. Song, "Design of a four-wheeled omnidirectional mobile robot with variable wheel arrangement mechanism," in *Proc. IEEE Int. Conf. Robot. Autom.*, vol. 1, May 2002, pp. 720–725.

[25] H. P. Oliveira, A. J. Sousa, A. P. Moreira, and P. J. Costa, "Modeling and assessing of omni-directional robots with three and four wheels," in *Proc. Contemp. Robot., Challenges Solutions*, 2009, pp. 207–229.

[26] C. Ren and S. Ma, "A continuous dynamic model for an omnidirectional mobile robot," in *Proc. IEEE Int. Conf. Robot. Autom. (ICRA)*, May/Jun. 2014, pp. 2919–2924.

[27] Y. Mori, E. Nakano, and T. Takahashi, "Mechanism, control and design methodology of the nonholonomic quasi-omnidirectional vehicle 'ODV9,'" *Int. J. Robot. Res.*, vol. 21, nos. 5–6, pp. 511–525, 2002.

[28] C. Stöger, A. Müller, and H. Gattringer, "Kinematic analysis and singularity robust path control of a non-holonomic mobile platform with several steerable driving wheels," in *Proc. IEEE/RSJ Int. Conf. Intell. Robots Syst. (IROS)*, Sep./Oct. 2015, pp. 4140–4145.

ZHIGUO LU received the B.E. and M.E. degrees from Northeastern University, Shenyang, China, in 2006 and 2008, respectively, and the Ph.D. degree from the Department of Micronano Systems Engineering, Nagoya University, Nagoya, Japan.

He is currently an Associate Professor with the School of Mechanical Engineering and Automation, Northeastern University. His research interests include hybrid position/force control, design of load adaptively underactuated mechanisms, and generation of energetically efficient robot motions.

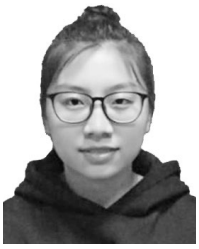

MENGLEI LIN was born in Nei Monggol Autonomous Region, China, in 1995. She received the B.S. degree in forest engineering from Northeast Forestry University, Harbin, in 2018. She is currently pursuing the master's degree with the School of Mechanical Engineering and Automation, Northeastern University, China. Her research interest includes motion planning of humanoid robot.

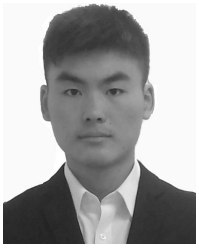

SHIXIONG WANG was born in Yunnan, China, in 1997. He received the bachelor's degree from the School of Mechanical Engineering and Automation, Northeastern University, China, in 2018, where he is currently pursuing the master's degree. His research interest includes mechanical structure design.

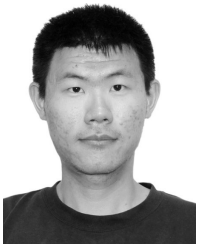

YICHEN ZHANG was born in Tianjin, China, in 1995. He received the B.S. degree from the School of Mechanical Engineering and Automation, Northeastern University, China, in 2017, where he is currently pursuing the master's degree. His research interests include image recognition technique, robot location, and navigation.

YONGJI YU received the B.S. degree in mechanical design, manufacturing, and automation from Shenyang Ligong University and the M.E. degree in mechanical design, manufacturing, and automation from the School of Mechanical Engineering and Automation, Northeastern University, in 2018. He is currently with Huawei Technologies Company Ltd., Shenzhen.